Engineering Chemistry
ISSN: 2813-6535, Vol. 3, pp 13-18
doi:10.4028/p-08k84g

Submitted: 2023-02-23
Accepted: 2023-03-12
Online: 2023-06-20

Synthesis and Characterization of Carbonate Hydroxyapatite from *Pinctada Maxima* Shell with Short Aging Time for Bone Biomaterial Candidate

Megawati Megawati[1,a], Diana Julaidy Patty[1,b] and Yusril Yusuf[1,c,*]

[1]Department of Physics, Faculty of Mathematics and Natural Science, Universitas Gadjah Mada, Yogyakarta, Indonesia

[a]megawati2020@mail.ugm.ac.id, [b]dianapatty.dp@mail.ugm.ac.id, [c]yusril@ugm.ac.id

Keywords: Carbonate hydroxyapatite, *P. maxima*, short aging time, bone biomaterial

Abstract. Biomaterial products for bone repair are needed to support accelerated tissue healing. This research aimed to synthesize and characterize carbonate hydroxyapatite (CHA) from *Pinctada maxima* (*P. maxima*) using the precipitation method with a short aging time, 15 min. CHA was dried with oven-dry at 100ºC for 12 h (CHA A) and a furnace-dry at 1000ºC for 2 h (CHA B). Short aging time succeeded in producing CHA B-type with lattice parameters a and c of CHA A is 9.382 Å and 6.964 Å, while 9.451 Å and 6.962 Å for CHA B. The high temperature treatment made the diffraction peak indicating CHA more detected and crystallinity increased to 97.87%. The appearance of C–O bond and diffraction peaks of CHA verified substituted carbonates hydroxyapatite.

Introduction

Bone is an important organ that supports the body and the attachment of muscles and organs. Bone consists of 50–70% inorganic mineral components, 20–40% organic, 5–10% water, and approximately 3% fat [1]. The main inorganic component of bone is the mineral hydroxyapatite (HA). HA has the chemical formula $Ca_{10}(PO_4)_6(OH)_2$ in the presence of small amounts of carbonate, magnesium, and phosphoric acid. Each HA unit cell has a hexagonal structure (Fig. 1.a) [2-4].

The carbonate content in bone is about 2–8% depending on the individual's age [5]. Carbonate that is substituted in the HA structure is called Carbonate Hydroxyapatite (CHA). The chemical formula is generally written as $(Ca_{10}(PO_4)_{6-x}(CO_3)_x(OH)_2$ indicated that unite cell CHA consist of phosphorus, carbonate, and calcium [6].

The carbonate ion can substitute for HA in three types. CHA A-type is the carbonate ion substituted on the hydroxyl ion (OH^-), CHA B-type on the phosphate ion (PO_4^{3-}), and CHA AB-type on the hydroxyl ion and phosphate ion [7]. CHA B-type is predominantly found in the body and is easier to synthesize because it can be carried out at low temperatures. CHA B-type a planar bivalent (CO_3^{2-}) that replaced (PO_4^{3-}) showed in Fig. 1.b.

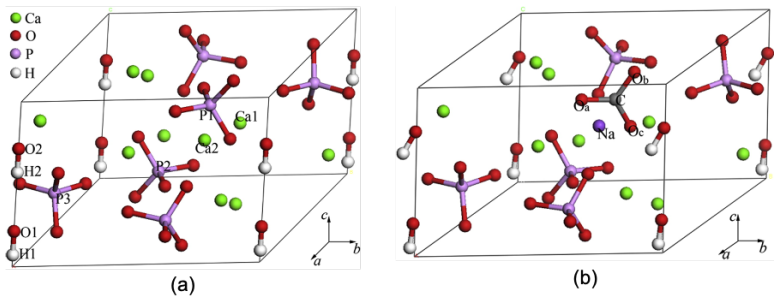

Figure 1. Chemical structure and unit cell of HA (a) and CHA B-type (b)[7].

P. maxima is a biogenic material candidate for the bone because it contains a lot of calcium [8]. The content of calcium carbonate in biogenic materials is quite significant, around 95-99% [5]. Calcium carbonate ($CaCO_3$) at high temperatures decomposed into calcium oxide (CaO) and carbon

gas (CO_2), as shown in Eq. (1). CaO can be used to synthesize biomaterials such as HA and CHA. CHA can be synthesized from biogenic materials such as egg shells, animal bones, fish bones, and shells.

$$CaCO_{3\,(s)} \rightarrow CaO_{(s)} + CO_{2(g)} \quad (1)$$

The precipitation method was used to synthesize CHA because it was easy to perform. Aging time is one of the important factors in the carbonate substitution process in the HA structure. Patty et. al., and Anggraini synthesized CHA from *P. maxima* uses the aging time of 24 h [9, 10]. Heating at high temperatures makes forming to produce substituted carbonates.

In this study, the synthesis of CHA was developed using a short aging time to shorten the synthesis time. The time of 15 minutes was chosen because the CHA constituent particles have settled after experiencing precipitation. The rapid aging process accompanied by annealing at high temperatures is expected to produce the desired CHA. CHA with carbonate content can be used for bone biomaterial applications because its composition resembles the natural condition of bone.

Material and Experimental Method

Material. The materials used for CHA synthesis were *P. maxima* shells, diammonium hydrogen phosphate ($(NH_4)_2.HPO_4$) (Sigma Aldrich), Ammonium bicarbonate (NH_4HCO_3) (Sigma Aldrich), ammonium hydroxide (NaOH) (Sigma Aldrich), and distilled water.

Experimental Method. The experimental process began with preparing the raw material, *P. maxima* shells. *P. maxima* shell was decomposed into CaO referring to previous research [9, 10]. CaO was used as a calcium source for CHA synthesis.

Preparation Sample. *P. maxima* shells were cleaned with water and soaked in acetone for 24 h. The raw were dried and cut into small pieces of approximately 1–2 cm. The pieces of shells were ball-milled and sieved. The raw powder was furnaced at 1000°C for 4 h and then sieved again using a 230 mesh (67 μm size particle) sieve to collect a homogeneous CaO.

Synthesis of CHA. Diammonium hydrogen phosphate $(NH_4)_2.HPO_4$ (7.05 g) was dissolved in 35 ml of distilled water and then stirred at 500 rpm for 30 min. Ammonium bicarbonate NH_4HCO_3 (4.48 g) was dissolved in 35 ml of distilled water and then stirred at 500 rpm for 30 min. The $(NH_4)_2.HPO_4$ solution was titrated using burette to NH_4HCO_3 solution with rate of approximately 1 ml/min.

CaO (5 g) decomposed from the *P. maxima* was dissolved in 50 ml of distilled water and then stirred at 500 rpm for 30 min. The titration result of $(NH_4)_2.HPO_4$ and NH_4HCO_3 solution titrated using burette to $Ca(OH)_2$ solution with rate of approximately 1 ml/min while stirring at 500 rpm in 80 ºC.

The pH solution was maintained at 10 by adding 3% NaOH. After titration, the solution was stirred and heated for up to 30 min until homogenous. The solution was aged for 15 min then filtered. The supernatant was dried in the oven at 100ºC for 12 h (CHA A) to remove moisture and annealed in furnaces at 1000ºC for 2 h (CHA B) to form the CHA structure more complete.

Characterization. The samples were characterized using Fourier transform infrared (FTIR) (Thermo Scientific Nicolet iS10) at the LPPT UGM Unit 1 with a range of wave number of 650–4000 cm^{-1} to determine functional vibrational groups. X-ray diffraction (XRD) (Shimadzu, R600) with CuKα 1.54060 Å was performed at the Chemistry Laboratory, FMIPA, UGM, to determine the crystal structure of CHA. Scanning electron microscope-energy dispersive X-ray (SEM-EDX) (JEOL, JSM-6510LA) was conducted at LPPT UGM to determine the morphology and content of CHA samples.

Results and Discussion

FTIR Spectra. The FTIR of CaO (Fig. 2.b) decomposition of raw *P. maxima* showed a sharp peak in the 3639 cm^{-1} indicating the stretching vibration of the O–H bond [11]. Absorption also appears at

1414 cm^{-1} indicating the presence of C–O bonds, while low absorption at 869 cm^{-1} indicates the presence of vibrations from Ca–O bonds [12]. The high temperature treatment made *P. maxima* decomposed, so the O–H bonds are more specific due to the contribution of Ca(OH) compounds.

The FTIR results of CHA showed absorption similar to previous studies (Fig. 2.a) [9]. CHA (Fig. 2.b) showed a sharp peak at 1013–1020 cm^{-1} region indicating vibration from P–O bond [13]. Absorbance at 1410 cm^{-1} and 872 cm^{-1} are stretching and bending vibrations of the C–O bond [14]. Absorbance also appeared at 3360 and 3640 cm^{-1} are characteristic vibrations of the O–H bond [5], [15].

The absorption indicating O–H in CHA A has a low absorption intensity at 3360 cm^{-1} while CHA B shifted to 3640 cm^{-1} with a higher and sharper intensity. This O–H bond contributes to the hydroxyl in the CHA structure. The presence of C–O absorption in CHA A indicates that oven-dry has succeeded in substituting carbonates into the CHA. After high temperature treatment (CHA B), O–H absorption sharped, then P–O bond intensity decreased. During high temperature treatment, the particles vibrated so that the carbonate could substitute the sample by replacing the phosphate position to form CHA B-type [5, 13, 16]. Presence absorbance of C–O, P–O, and O–H bonds like structure of CHA in Fig. 1.b indicated that CHA has successfully formed.

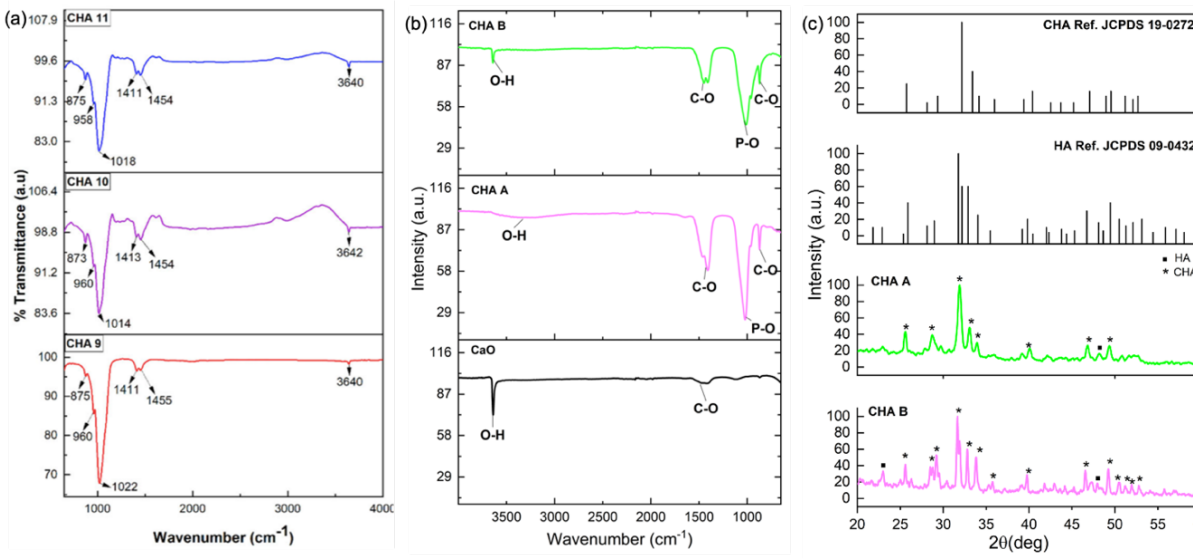

Figure 2. FTIR of CHA from previous studies [9] (a), FTIR sample CaO, CHA A, and CHA B (b), and diffraction of CHA A and CHA B.

X-Ray Diffraction. The structure of CHA has similarities with HA which has main peaks at the *hkl* index 25.87° (002), 32.19° (211), and 32.90° (300) according to JCPDS 09-0432 and CHA B-type at JCPDS 19-0272. CHA A has diffraction at 2θ angle positions 25.55° (002), 28.64° (210), 31.89° (211), 33.04° (300), 33.90° (202), 40.02° (310), 46.77° (222), 48.14° (312), and 49.31° (213). These peaks indicate the formation of the CHA structure.

CHA B has diffraction at 2θ angle positions 22.96° (111), 25.56° (002), 28.47° (102), 29.18 (210), 31.63° (211), 31.90° (300), 33.80° (202), 35.72 (301), 39.72° (310), 46.53° (222), 47.93° (312), 49.21° (213), 51.17° (231), 51.94° (410), 52.77° (402), and 55.74° (004). The main diffraction peak formed in CHA shifted from the diffraction peak HA indicating the presence of carbonate ion substitution in the HA structure [13]. The high temperature heating process makes more diffraction peaks and the width between the diffraction peaks gets narrower. The narrower peak indicates the better CHA structure. The presence of carbonate substitution makes the peaks at (211) and (300) coincide each other.

Table 1 the results from the XRD diffraction analysis data using data on the main diffraction peaks. CHA A has lattice parameters a and c of 9.382 Å and 6.964 Å, respectively, while CHA B is 9.451 Å and 6.962 Å. CHA A and CHA B have a larger lattice parameter c than the reference HA, while the lattice parameter a CHA A is smaller. This condition is appropriate with the characteristic of CHA

B-type, where the lattice parameter a is smaller while the parameter c is larger than the HA reference [6, 13].

Table 1. XRD parameter of CHA.

Sample	Lattice parameter (Å)		c/a	Crystallite size, L (nm)	Volume unit cell, V (g/cm^3)	Microstrain, ϵ (°)	Crystallinity, X_c (%)
	a	c					
HA Ref.	9.418	6.884	0.730	-	-	-	-
CHA A	9.382	6.964	0.743	26.09	1592.334	0.006	95.37
CHA B	9.451	6.962	0.736	45.09	1615.644	0.004	97.87

The lattice parameter $\frac{1}{d^2} = \frac{4}{3}\left(\frac{h^2+hk+l^2}{a^2}\right) + \frac{l^2}{c^2}$; crystallite size $(L) = \frac{k\lambda}{\beta \cos\theta}$; Volume unit cell $(V) = \frac{3\sqrt{3}}{2}a^2c$; microstrain $(\epsilon) = \frac{FWHM}{4\tan\theta}$; and crystallinity $(X_c) = 1 - \left(\frac{V_{211/300}}{I_{300}}\right)$; FWHM is the full width at half maximum.

The annealing process at 1000 °C for 2 h caused the particles forming the CHA to vibrate and integrate to form the CHA structure. During the annealing process, the carbonate ion undergoes substitution to replace the phosphate ion position. This situation makes the lattice parameter a decrease while the lattice parameter c increases so that the ratio parameter $(\frac{c}{a})$ of CHA B to be closer to the value of the reference than CHA A.

High-temperature treatment makes the micro and nano grains of HA to be integrated and makes the particles experience compaction. This makes the crystallite size in CHA B increased to 45.09 nm, while the volume unit cell increased to 1615.644 g/cm^3 compared to CHA A. A low microstrain was detected at 0.006° and 0.004°, which indicated a very small crystal defect [11]. The crystallinity of furnace-dried CHA is higher than that of oven-dried CHA up to 97.87%.

The diffraction peaks indicated the presence of CHA with lattice parameters a decreased and c increased indicating that the synthesis was confirmed to CHA B-type. This result is strengthened by the FTIR result, which confirmed the presence of C–O, P–O, and O–H bonds.

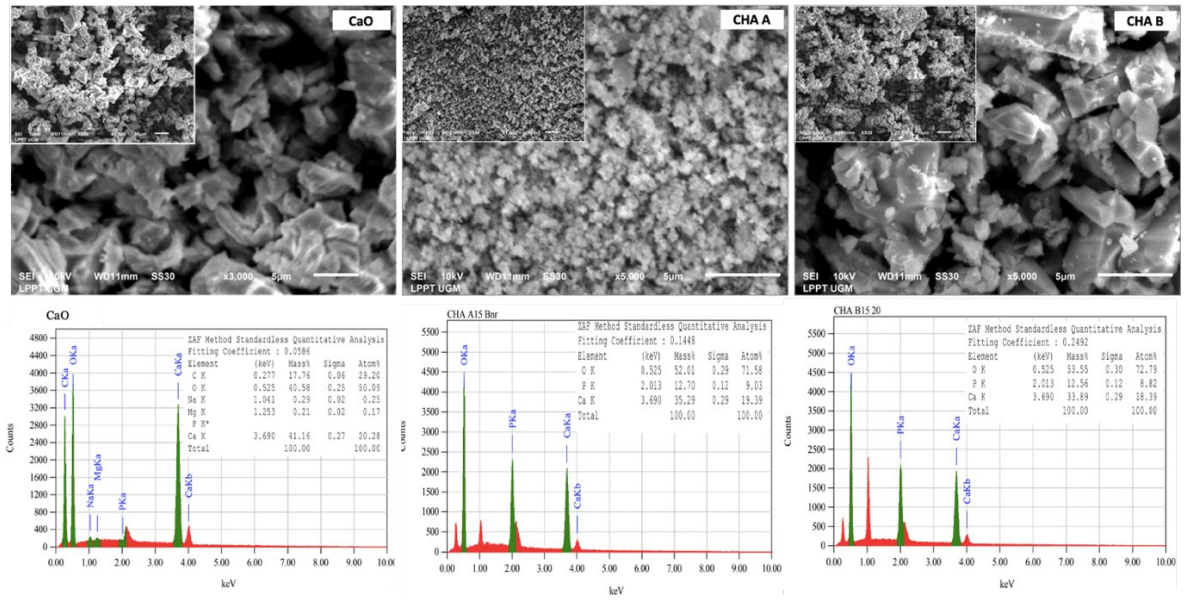

Figure 3. Morphology and content from SEM-EDX result of CaO, CHA A, and CHA B.

Morphology Properties. The SEM and EDX result of CaO and CHA results are shown in Fig. 3. The CaO has solid particles. The EDX results show that the main content is calcium up to 41.16% and carbon as much as 17.76%. This high calcium content supports its use as the main ingredient in the synthesis of CHA.

CHA A showed uniform grains with grain sizes of approximately 0.01–0.1 μm. High temperature treatment made the morphology of CHA B has an irregular square shape with a slick surface. The grain diameter of approximately 0.5–2 μm. This result is confirmed by the FTIR and XRD results

analysis previously which reported that after high temperature treatment, CHA is more detected and indicating carbonate substituted in the HA structure.

Table 2. Molar ratio of CHA.

Sample	Ca (%)	P (%)	n Ca (mol)	n P (mol)	Ratio* (Ca/P)
CHA A	35.29	12.70	0.88	0.41	2.15
CHA B	33.89	12.56	0.85	0.41	2.09

*Molar ratio $\left(\frac{Ca}{P}\right) = \frac{mass\ Ca}{Ar\ Ca}\ x\ \frac{mass\ P}{Ar\ P}$; Ar Ca = 40 and P = 31

The EDX results showed that all CHA samples contained calcium and phosphate. The molar ratio (Ca/P) of CHA is presented in Table 2. The calcium and phosphate content in CHA A was higher than CHA B so ratio (Ca/P) of CHA A is 2.15 while CHA B is 2.09. High temperature treatment causes the calcium and phosphate content decreased. This condition happened because the carbonate substituted in the phosphate site, so the phosphate content decreased then (Ca/P) in CHA was higher than HA.

This result is also validated by the FTIR results of CHA which showed the absorption intensity of P–O bonds decreased while C–O bonds increased. The XRD results also showed lattice parameter a decreased while lattice parameter c increased indicating CHA B-type. The results of CHA B-type are similar to the results of the previous CHA which can be used for bone repair such scaffold in bone tissue engineering [9].

Summary

CHA synthesized from *P. maxima* with short aging time of 15 min succeeded has major diffraction peaks (002), (211), and (300) indicating the formation of a CHA structure. CHA A had lattice parameters a and c are 9.382 Å and 6.964 Å, while CHA B was 9.451 Å and 6.962 Å that indicating CHA B-type. The substituted carbonate was evident from the presence of FTIR absorption at 1410 cm^{-1} and 872 cm^{-1} indicating the C–O bond. CHA A has ratio (Ca/P) is 2.15 while CHA B is 2.09 occurs because of the carbonate content in the CHA. The high temperature treatment increased crystallite size increased up to 45.09 nm and crystallinity up to 97.87%. This result indicates that synthetic CHA can be used for applications in biomaterials such as bone repair.

Acknowledgements

The authors would like to thank the Ministry of Education, Culture, Research, and Technology, Republic of Indonesia, for the PTM Grant (1956/UN1/DITLIT/Dit-Lit/PT.01.03/2022) and the Indonesian Endowment Fund for Education (KET-78/LPDP.3/2022) for financial support, and the Laboratory of Material Physics and Electronics, Integrated Research and Testing Laboratory at the University Gadjah Mada, Indonesia.

References

[1] A. Ressler, A. Žužić, I. Ivanišević, N. Kamboj, and H. Ivanković, "Ionic substituted hydroxyapatite for bone regeneration applications: A review," *Open Ceram.*, vol. 6, p. 100122, Jun. 2021, doi: 10.1016/j.oceram.2021.100122.

[2] J. Anita Lett *et al.*, "Recent advances in natural polymer-based hydroxyapatite scaffolds: Properties and applications," *Eur. Polym. J.*, vol. 148, no. October 2020, p. 110360, Apr. 2021, doi: 10.1016/j.eurpolymj.2021.110360.

[3] M. R. Mohd Roslan *et al.*, "The State of Starch/Hydroxyapatite Composite Scaffold in Bone Tissue Engineering with Consideration for Dielectric Measurement as an Alternative Characterization Technique," *Materials (Basel).*, vol. 14, no. 8, p. 1960, Apr. 2021, doi: 10.3390/ma14081960.

[4] S. Pai, M. S. Kini, and R. Selvaraj, "A review on adsorptive removal of dyes from wastewater by hydroxyapatite nanocomposites," *Environ. Sci. Pollut. Res.*, vol. 28, no. 10, pp. 11835–11849, Mar. 2021, doi: 10.1007/s11356-019-07319-9.

[5] R. Wati and Y. Yusuf, "Carbonated Hydroxyapatite Derived from Cerastoderma edule, Paphia undulata, and Meretrix meretrix Shells," *IOP Conf. Ser. Mater. Sci. Eng.*, vol. 546, no. 4, p. 042049, Jun. 2019, doi: 10.1088/1757-899X/546/4/042049.

[6] A. S. Khan and A. A. Chaudhry, *Handbook of Ionic Substituted Hydroxyapatites*. Elsevier, 2020.

[7] F. Ren, X. Lu, and Y. Leng, "Ab initio simulation on the crystal structure and elastic properties of carbonated apatite," *J. Mech. Behav. Biomed. Mater.*, vol. 26, pp. 59–67, Oct. 2013, doi: 10.1016/j.jmbbm.2013.05.030.

[8] D. J. Patty, A. D. Nugraheni, I. D. Ana, and Y. Yusuf, "In vitro bioactivity of 3D microstructure hydroxyapatite/collagen based-egg white as an antibacterial agent," *J. Biomed. Mater. Res. Part B Appl. Biomater.*, pp. 1–13, Jan. 2022, doi: 10.1002/jbm.b.35009.

[9] D. J. Patty, A. D. Nugraheni, I. D. Ana, and Y. Yusuf, "Dual functional carbonate-hydroxyapatite nanocomposite from Pinctada maxima and egg-white for bone tissue engineering," *J. Biomater. Sci. Polym. Ed.*, vol. 33, no. 8, pp. 1043–1062, May 2022, doi: 10.1080/09205063.2022.2036934.

[10] R. M. Anggraini and Y. Yusuf, "The Effect of Stirring Time on the Characteristics of Carbonated Hydroxyapatite from Pearl Shells (Pinctada maxima)," in *IOP Conference Series: Materials Science and Engineering*, 2019, vol. 546, no. 4, doi: 10.1088/1757-899X/546/4/042002.

[11] Y. Rizkayanti and Y. Yusuf, "Optimization of the temperature synthesis of hydroxyapatite from indonesian crab shells," *Int. J. Nanoelectron. Mater.*, vol. 12, no. 1, pp. 85–92, 2019, doi: 123456789/58781.

[12] I. Pawarangan and Y. Yusuf, "Characteristics of hydroxyapatite from buffalo bone waste synthesized by precipitation method," *IOP Conf. Ser. Mater. Sci. Eng.*, vol. 432, p. 012044, Nov. 2018, doi: 10.1088/1757-899X/432/1/012044.

[13] M. Kwaśniak-Kominek, M. Manecki, J. Matusik, and M. Lempart, "Carbonate substitution in lead hydroxyapatite Pb5(PO4)3OH," *J. Mol. Struct.*, vol. 1147, pp. 594–602, 2017, doi: 10.1016/j.molstruc.2017.06.111.

[14] I. K. Januariyasa and Y. Yusuf, "Porous carbonated hydroxyapatite-based scaffold using simple gas foaming method," *J. Asian Ceram. Soc.*, vol. 8, no. 3, pp. 634–641, Jul. 2020, doi: 10.1080/21870764.2020.1770938.

[15] R. M. Anggraini, A. I. Supii, G. B. Suparta, and Y. Yusuf, "The Effect of pH on the Characteristics of Carbonate Hydroxyapatite Based on Pearl Shell (*Pinctada maxima*)," *Key Eng. Mater.*, vol. 818, pp. 44–49, Aug. 2019, doi: 10.4028/www.scientific.net/KEM.818.44.

[16] A. Ressler, A. Žužić, I. Ivanišević, N. Kamboj, and H. Ivanković, "Ionic substituted hydroxyapatite for bone regeneration applications: A review," *Open Ceram.*, vol. 6, no. March, 2021, doi: 10.1016/j.oceram.2021.100122.